Supplemental Material

Journal of Climate
Two-Year Dynamical Predictions of ENSO Event Duration during 1954–2015
https://doi.org/10.1175/JCL-D-20-0619.1

Supplemental Online Materials for

"Two-year Dynamical Predictions of ENSO Event Duration during 1954-2015"

Xian Wu and Yuko M. Okumura

Institute for Geophysics, Jackson School of Geosciences

The University of Texas at Austin, Austin, TX

Clara Deser

Climate and Global Dynamics Division,

National Center for Atmospheric Research, Boulder, CO

Pedro N. DiNezio

Department of Atmospheric and Oceanic Sciences,

University of Colorado Boulder, Boulder, CO

Journal of Climate

Submitted August 04, 2020

Revised December 31 2020

Revised February 7, 2021

Corresponding author address: Dr. Xian Wu, Climate and Global Dynamics Division, National Center for Atmospheric Research, 1850 Table Mesa Drive, Boulder, Colorado, 80305

Email: xianwu@ucar.edu

Figure S1. As in Fig. 1, but for all other 1-yr El Niño (1963, 1965, 1982, 1991, 1994, 1997, 2002, 2006, and 2009), 2-yr El Niño (1957, 1968, 1976, and 2014), 1-yr La Niña (1964, 1995, and 2005), and 2-yr La Niña (1954, 1970, 1973, 1983, 2007, 2010, and 2016) events. The Nov^{-1} (Mar^{0}–Jun^{+1}) forecasts are not available for the 2-yr La Nina event that develops in 1954 (2016).

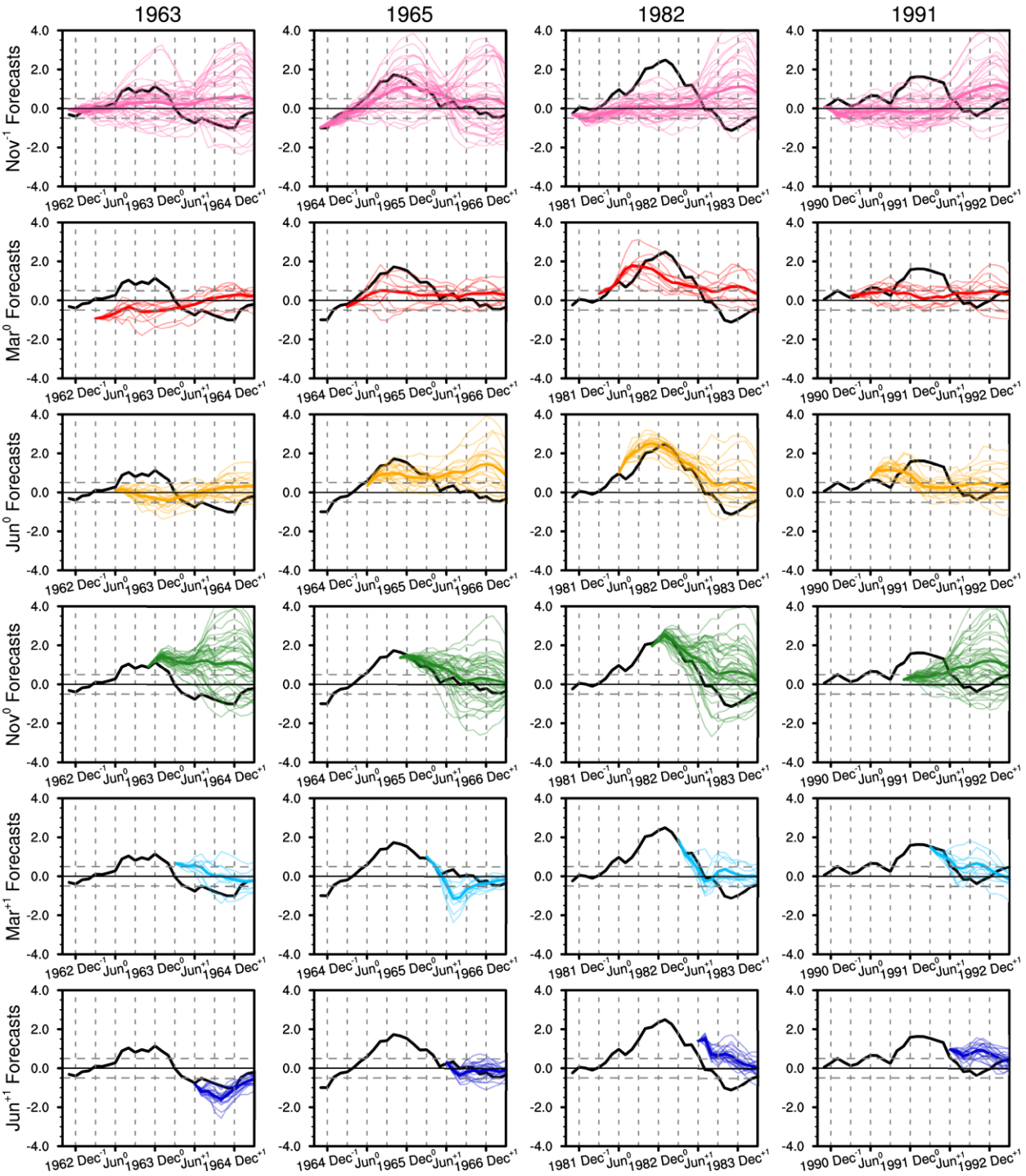

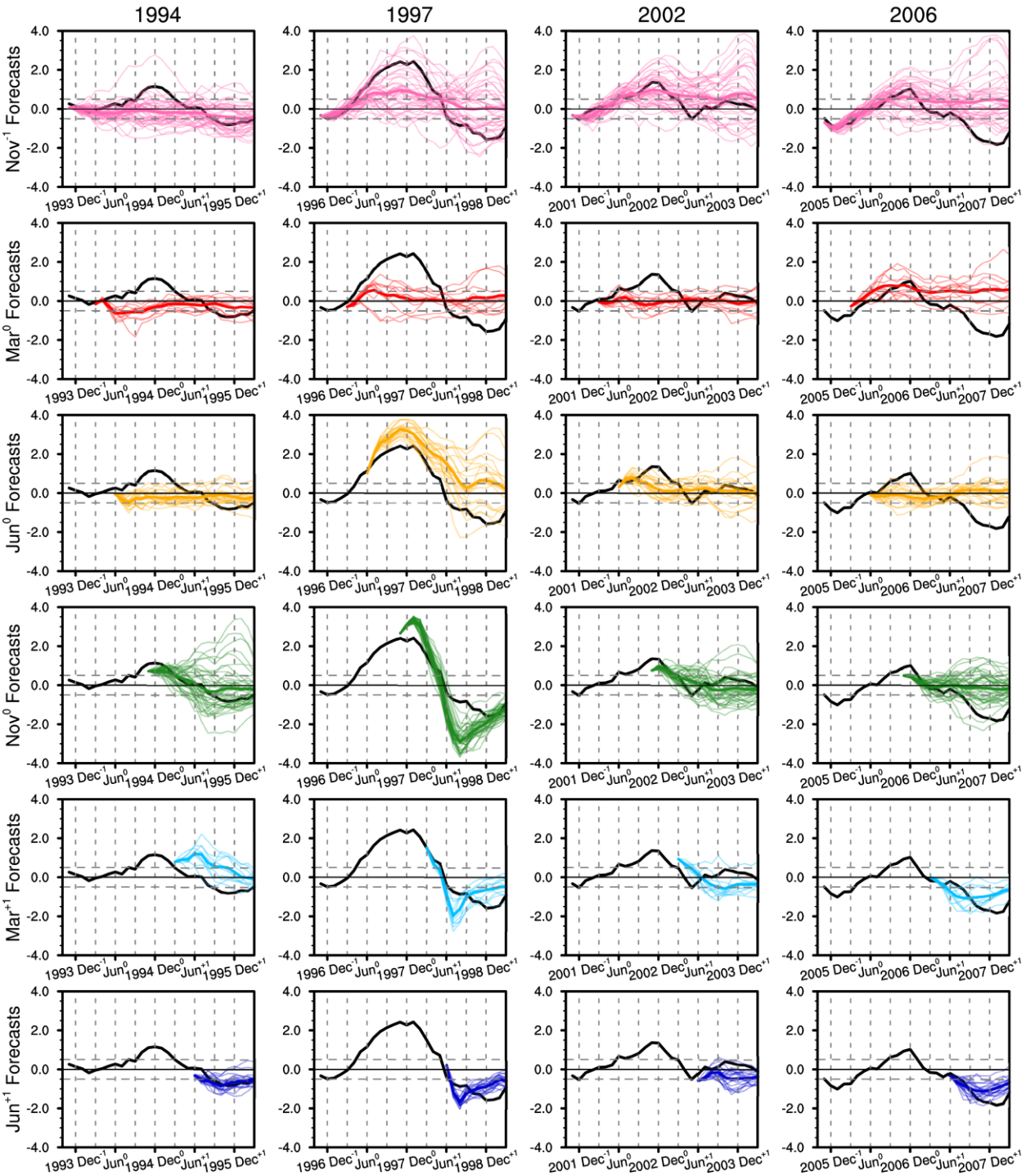
1994
1997
2002
2006
Nov-1 Forecasts
Mar0 Forecasts
Jun0 Forecasts
Nov0 Forecasts
Mar+1 Forecasts
Jun+1 Forecasts
4.0
2.0
0.0
-2.0
-4.0
1993 Dec-1 Jun0 1994 Dec0 Jun+1 1995 Dec+1
1996 Dec-1 Jun0 1997 Dec0 Jun+1 1998 Dec+1
2001 Dec-1 Jun0 2002 Dec0 Jun+1 2003 Dec+1
2005 Dec-1 Jun0 2006 Dec0 Jun+1 2007 Dec+1

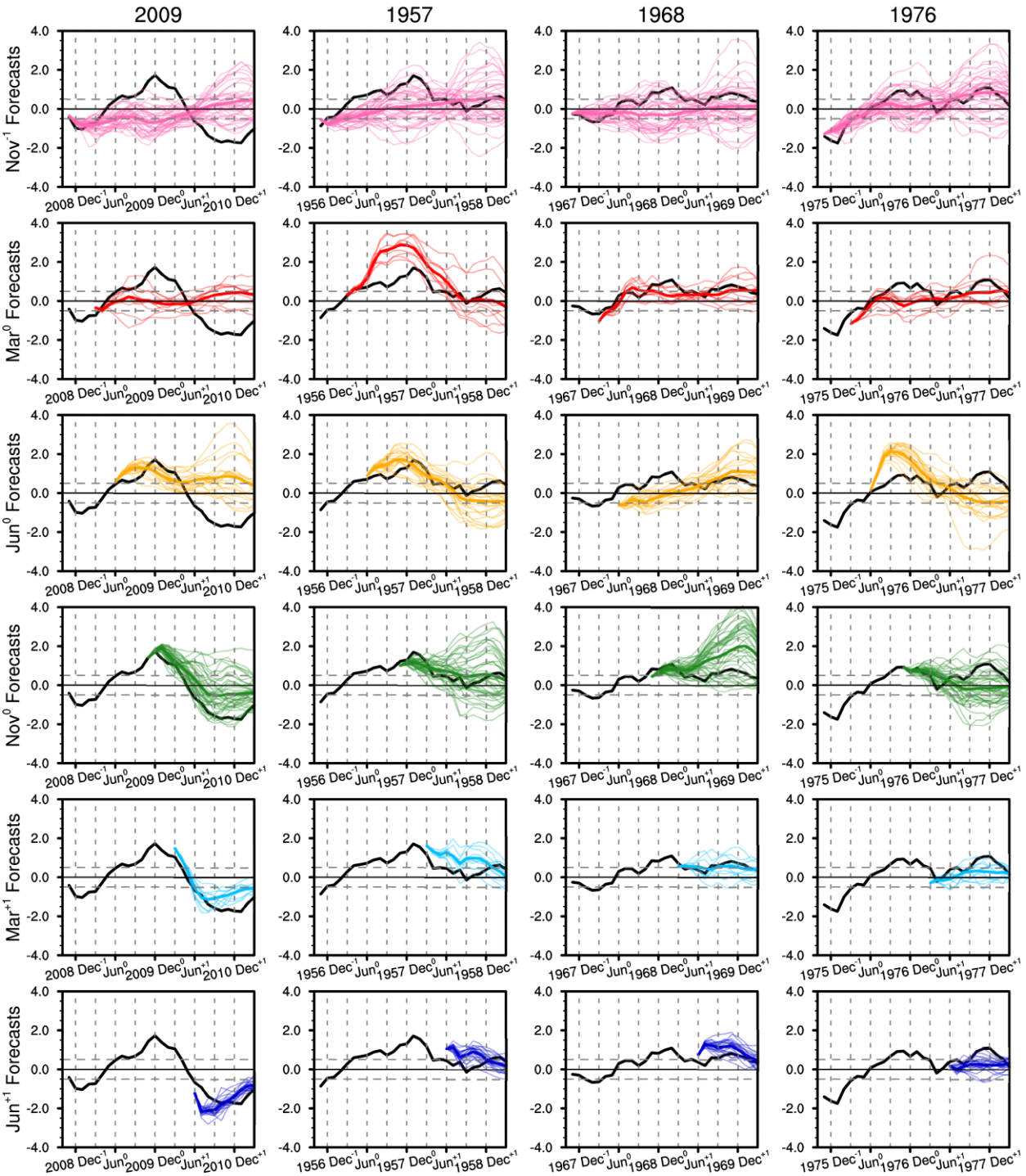
2009
1957
1968
1976
Nov-1 Forecasts
Mar0 Forecasts
Jun0 Forecasts
Nov0 Forecasts
Mar+1 Forecasts
Jun+1 Forecasts
4.0
2.0
0.0
-2.0
-4.0
2008 Dec-1 Jun0 2009 Dec0 Jun+1 2010 Dec+1
1956 Dec-1 Jun0 1957 Dec0 Jun+1 1958 Dec+1
1967 Dec-1 Jun0 1968 Dec0 Jun+1 1969 Dec+1
1975 Dec-1 Jun0 1976 Dec0 Jun+1 1977 Dec+1

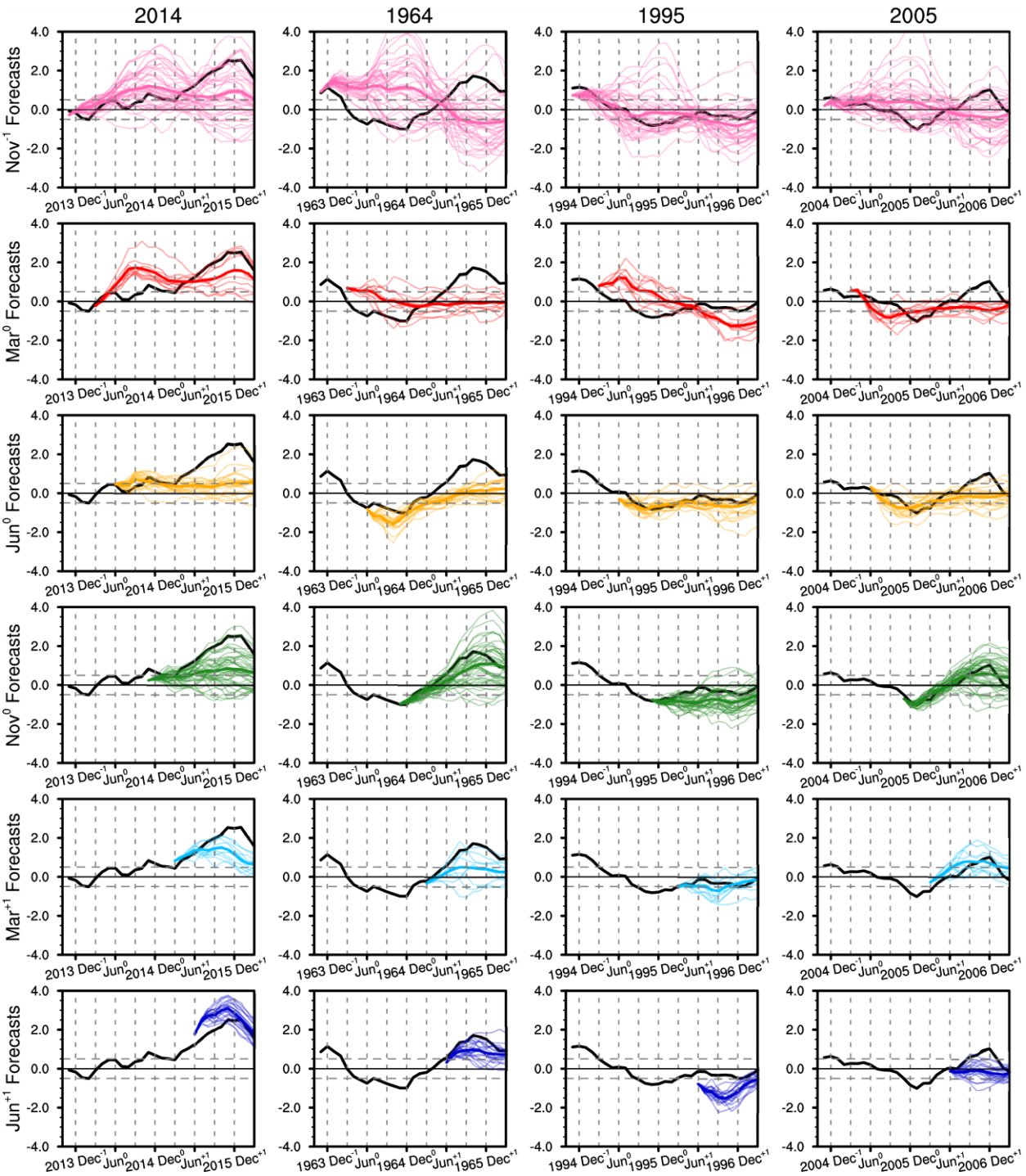
2014
1964
1995
2005
Nov-1 Forecasts
Mar0 Forecasts
Jun0 Forecasts
Nov0 Forecasts
Mar+1 Forecasts
Jun+1 Forecasts
4.0
2.0
0.0
-2.0
-4.0
2013 Dec-1 Jun0 2014 Dec0 Jun+1 2015 Dec+1
1963 Dec-1 Jun0 1964 Dec0 Jun+1 1965 Dec+1
1994 Dec-1 Jun0 1995 Dec0 Jun+1 1996 Dec+1
2004 Dec-1 Jun0 2005 Dec0 Jun+1 2006 Dec+1

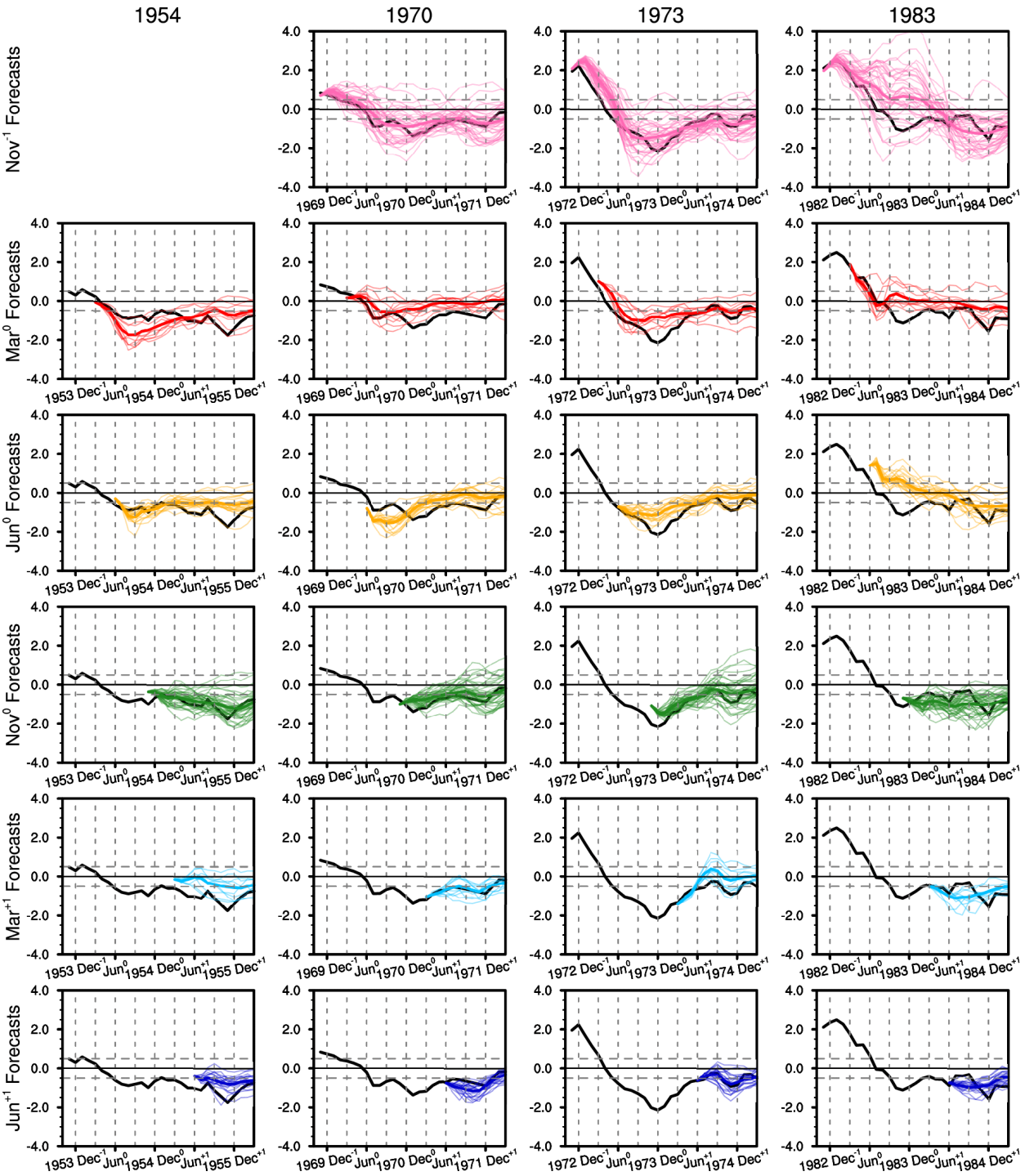
1954
1970
1973
1983
Nov-1 Forecasts
Mar0 Forecasts
Jun0 Forecasts
Nov0 Forecasts
Mar+1 Forecasts
Jun+1 Forecasts
4.0
2.0
0.0
-2.0
-4.0
1953 Dec-1 Jun0 1954 Dec0 Jun+1 1955 Dec+1
1969 Dec-1 Jun0 1970 Dec0 Jun+1 1971 Dec+1
1972 Dec-1 Jun0 1973 Dec0 Jun+1 1974 Dec+1
1982 Dec-1 Jun0 1983 Dec0 Jun+1 1984 Dec+1

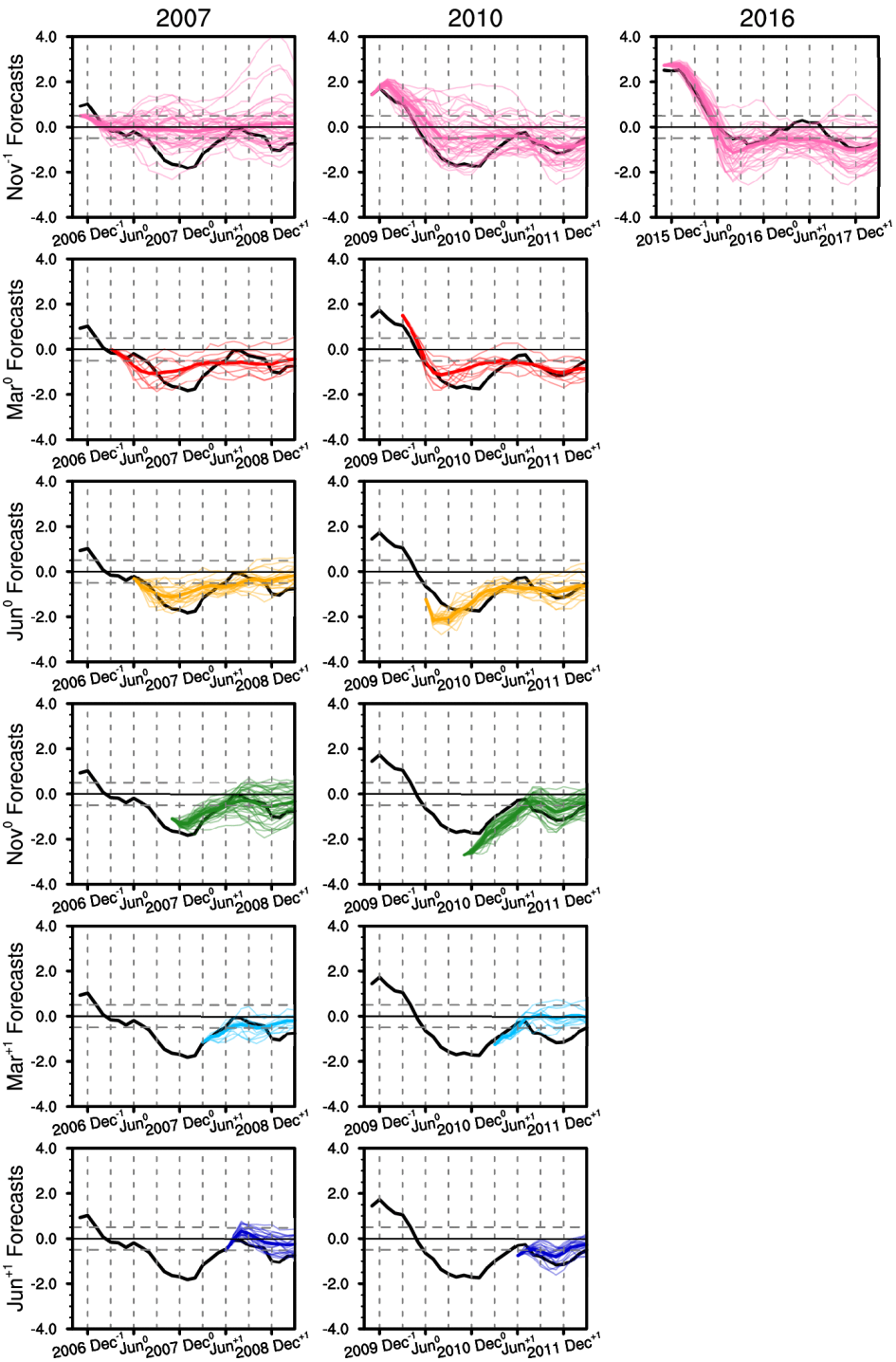
2007
2010
2016
Nov-1 Forecasts
Mar0 Forecasts
Jun0 Forecasts
Nov0 Forecasts
Mar+1 Forecasts
Jun+1 Forecasts
4.0
2.0
0.0
-2.0
-4.0
2006 Dec-1 Jun0 2007 Dec0 Jun+1 2008 Dec+1
2009 Dec-1 Jun0 2010 Dec0 Jun+1 2011 Dec+1
2015 Dec-1 Jun0 2016 Dec0 Jun+1 2017 Dec+1

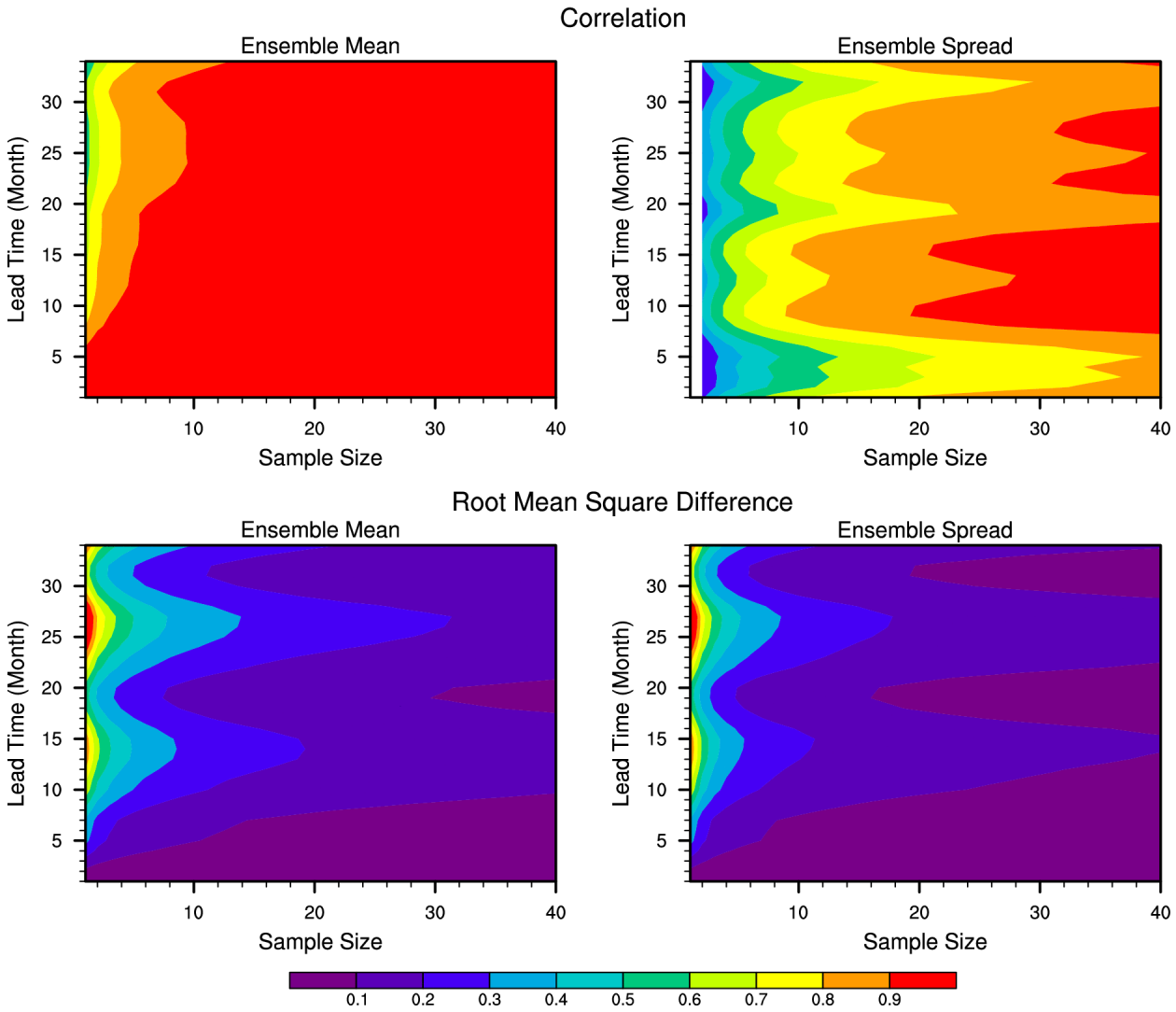

Figure S2. Average (top) correlation coefficient and (bottom) root-mean-square-difference (°C) of (left) ensemble mean and (right) ensemble spread between the 40-member ensemble of the Nov-initialized forecasts and 10,000 bootstrapped ensembles of 1 to 40 members of the Nov-initialized forecasts. The x-axis denotes the size of bootstrapped ensembles, and the y-axis denotes the forecast lead time (month) from the initialization month November.

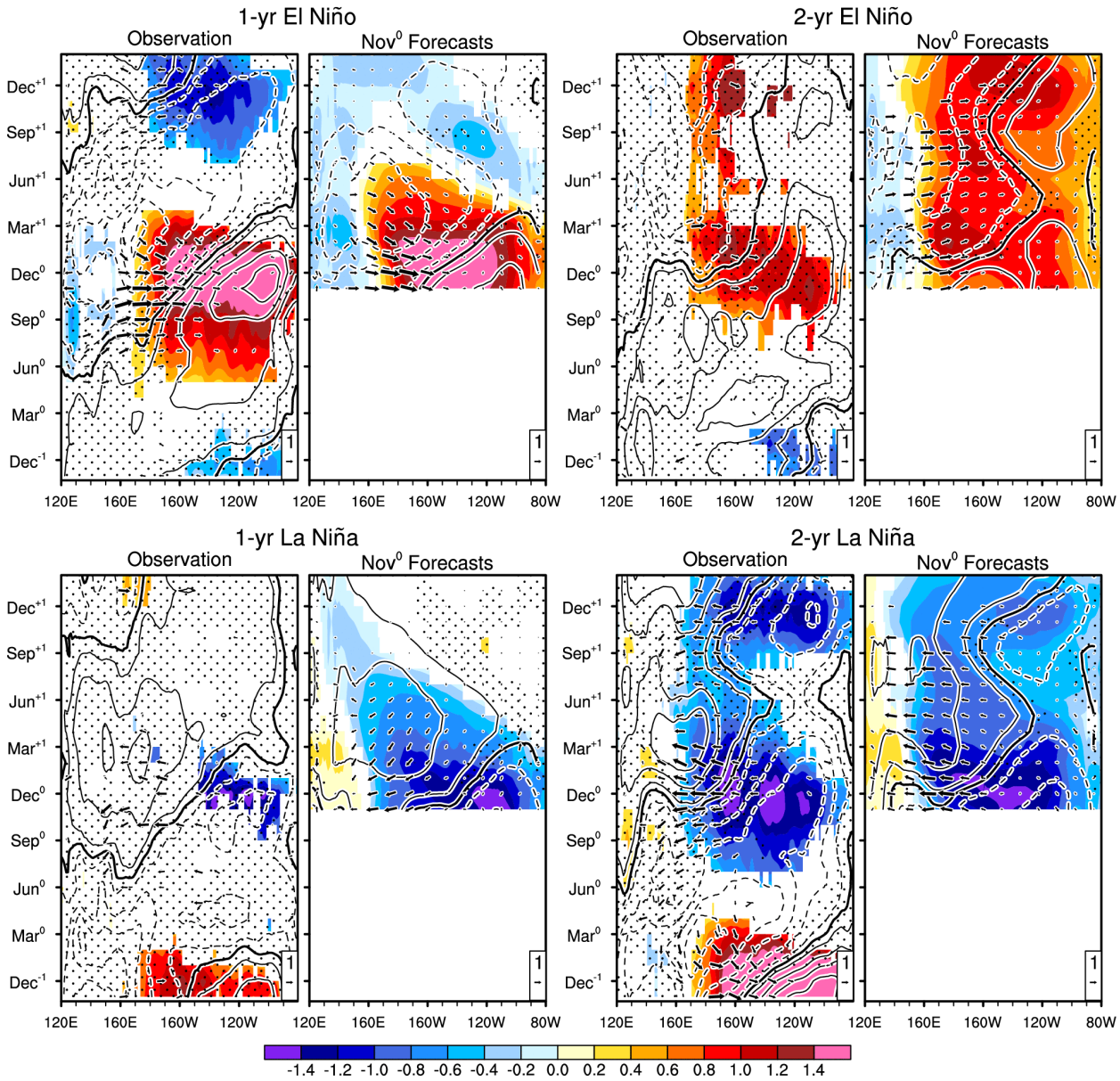

Figure S3. As in Fig. 5, but only SST and surface wind anomalies statistically significant at the 95% confidence levels are shown. The insignificant thermocline depth anomalies are masked by stipples.

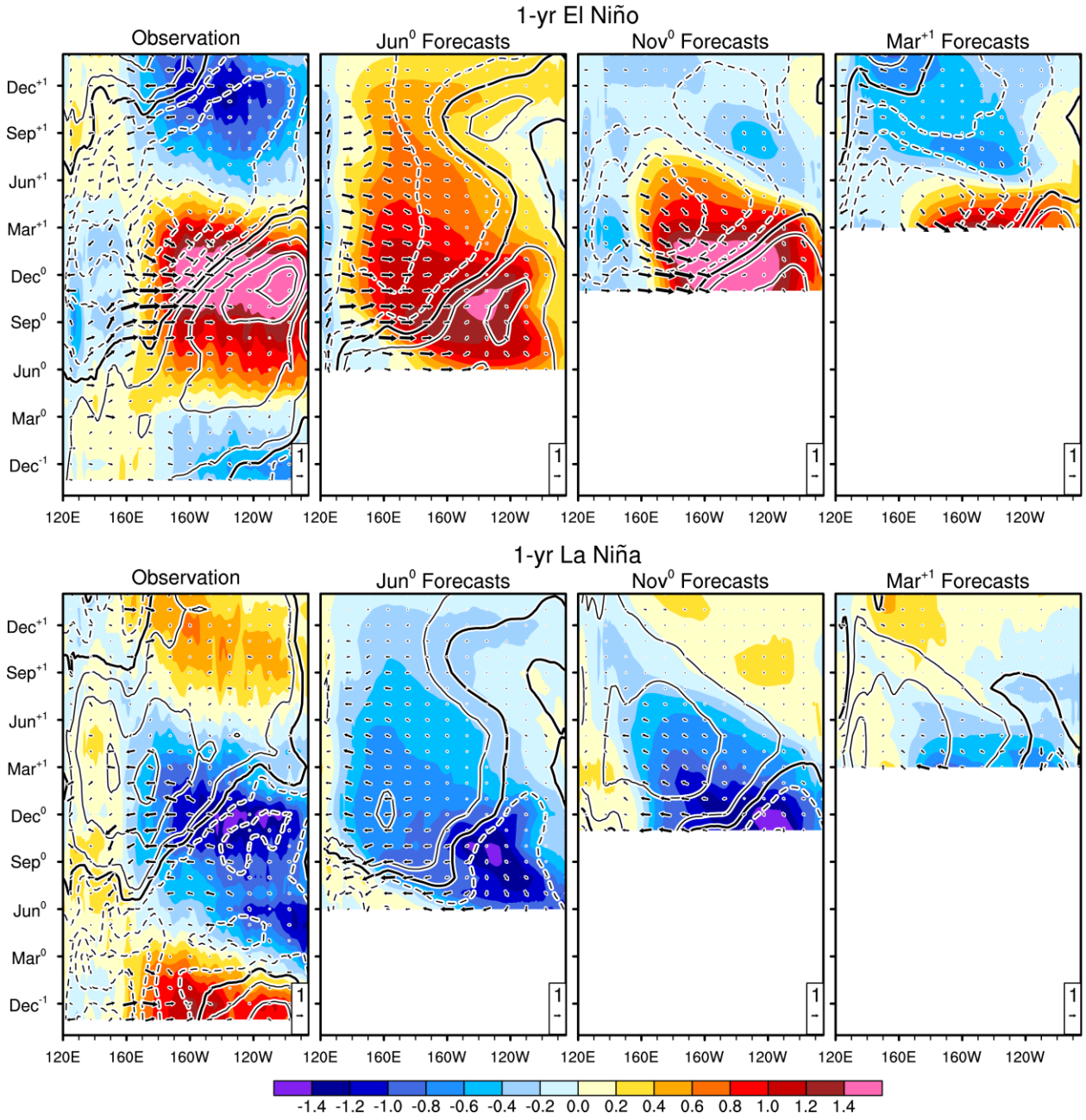

Figure S4. Longitude-time sections of SST (°C; shading), thermocline depth (contours at intervals of 8 m starting at ±4 m; zero contours thickened and negative contours dashed), and surface wind (m s^{-1}; vectors) anomalies in the equatorial Pacific (3°S–3°N) composited for 1-yr (top) El Niño and (bottom) La Niña events in (first column) observations and (second–fourth columns) ensemble forecasts initialized in (second column) Jun^0, (third column) Nov^0, and (fourth column) Mar^{+1}. The thermocline depth anomalies are smoothed with a 1-2-1 filter in the time direction and a 9-point running-mean filter in the longitudinal direction in both observations and forecasts.

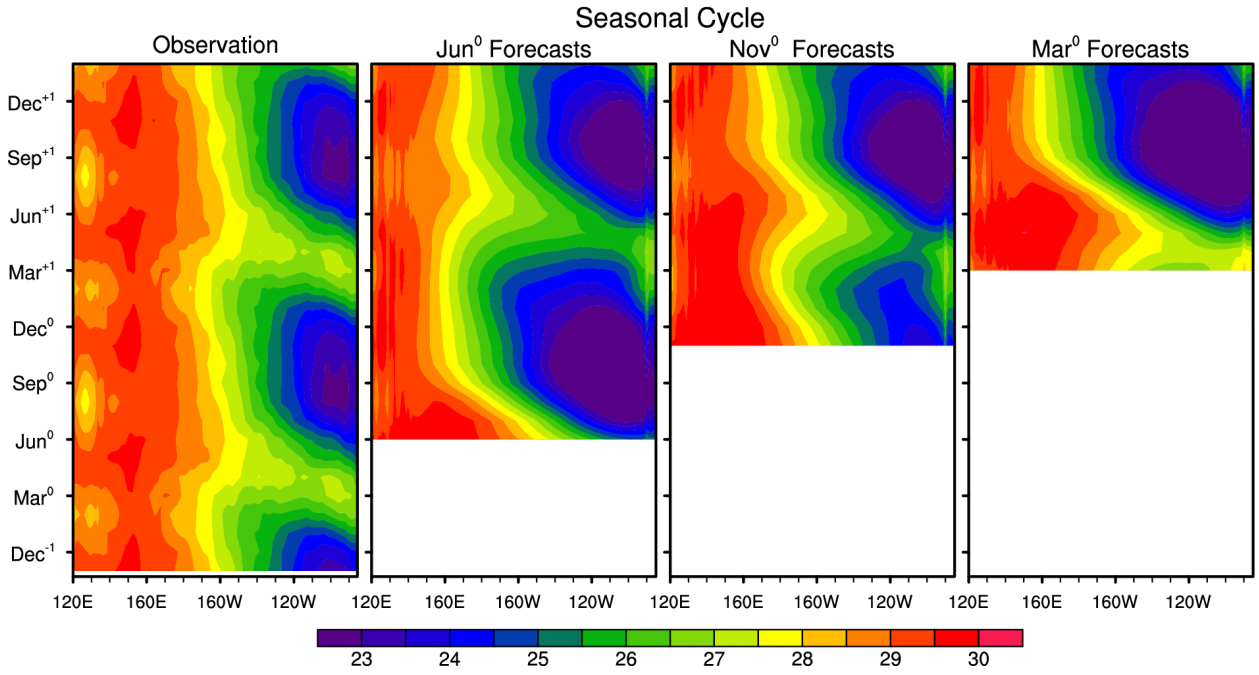

Figure S5. Longitude-time sections of climatological SST (°C; shading) in the equatorial Pacific (3°S–3°N) in observations and ensemble forecasts initialized in Jun^{0}, Nov^{0}, and Mar^{+1}. Note that the climatology in the forecasts is a function of lead time.

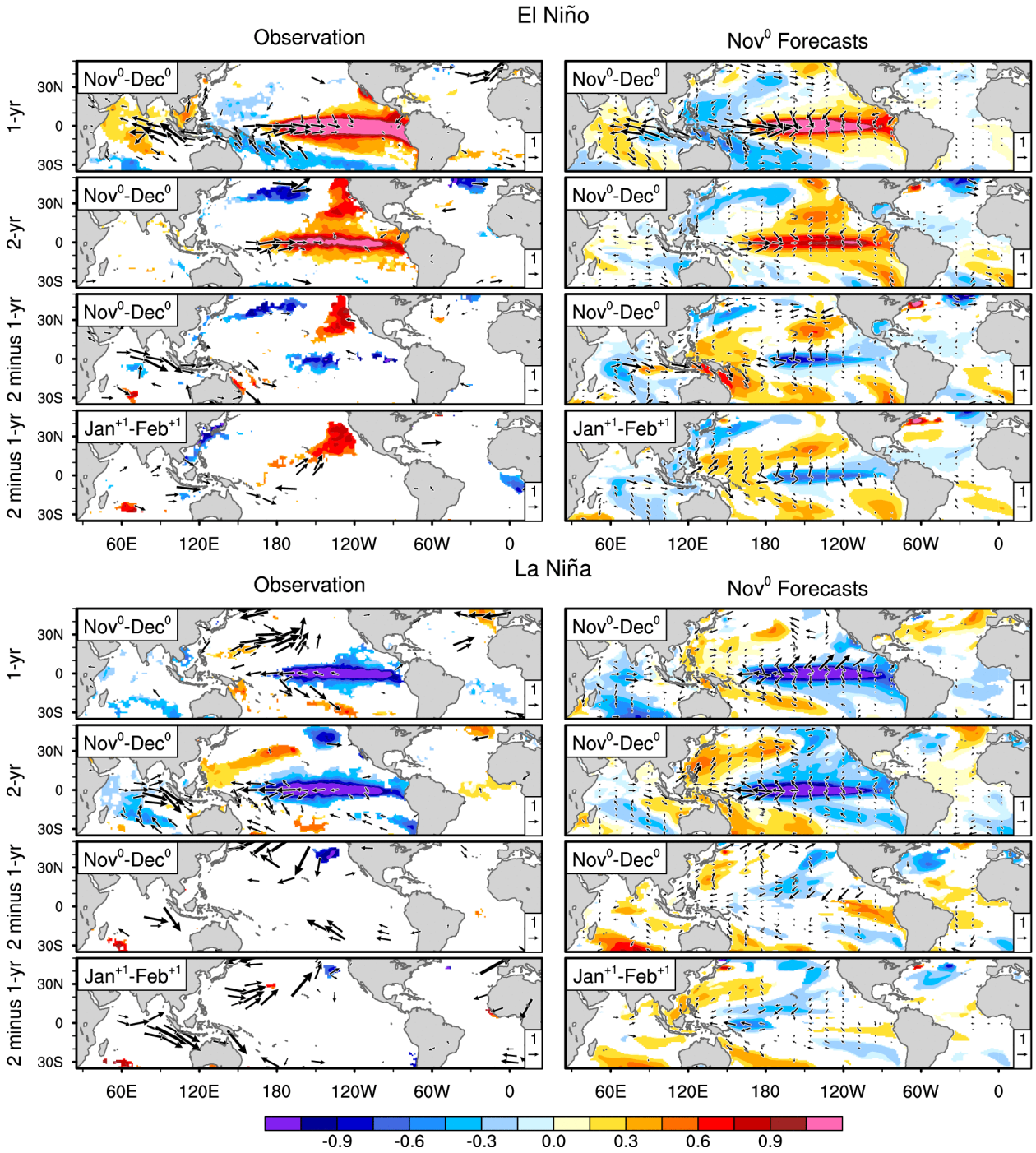

Figure S6. As in Fig. 6, but only SST and surface anomalies statistically significant at the 95% confidence levels are shown.

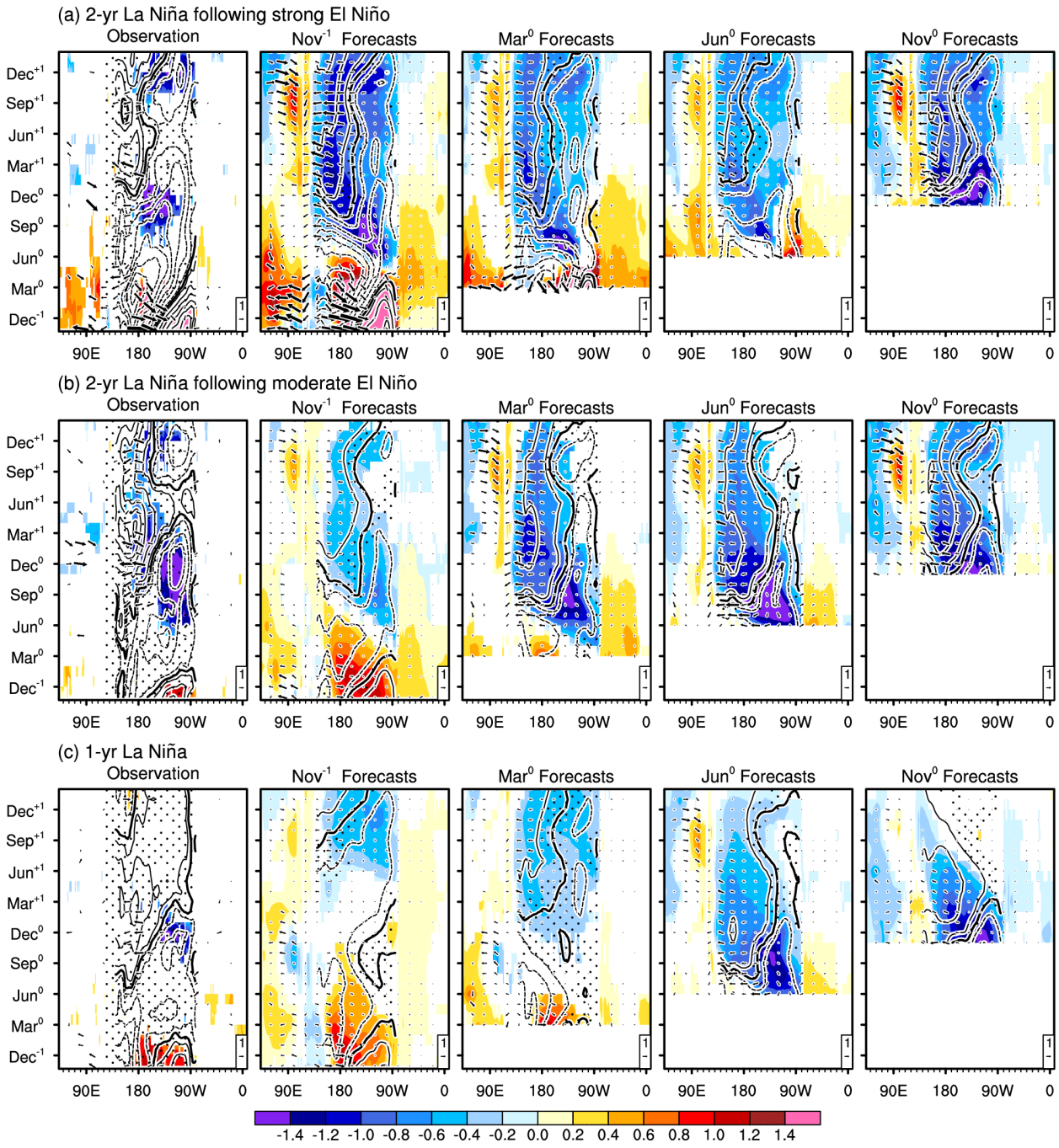

Figure S7. As in Fig. 8, but only SST and surface wind anomalies statistically significant at the 95% confidence levels are shown. The insignificant thermocline depth anomalies are masked by stipples.

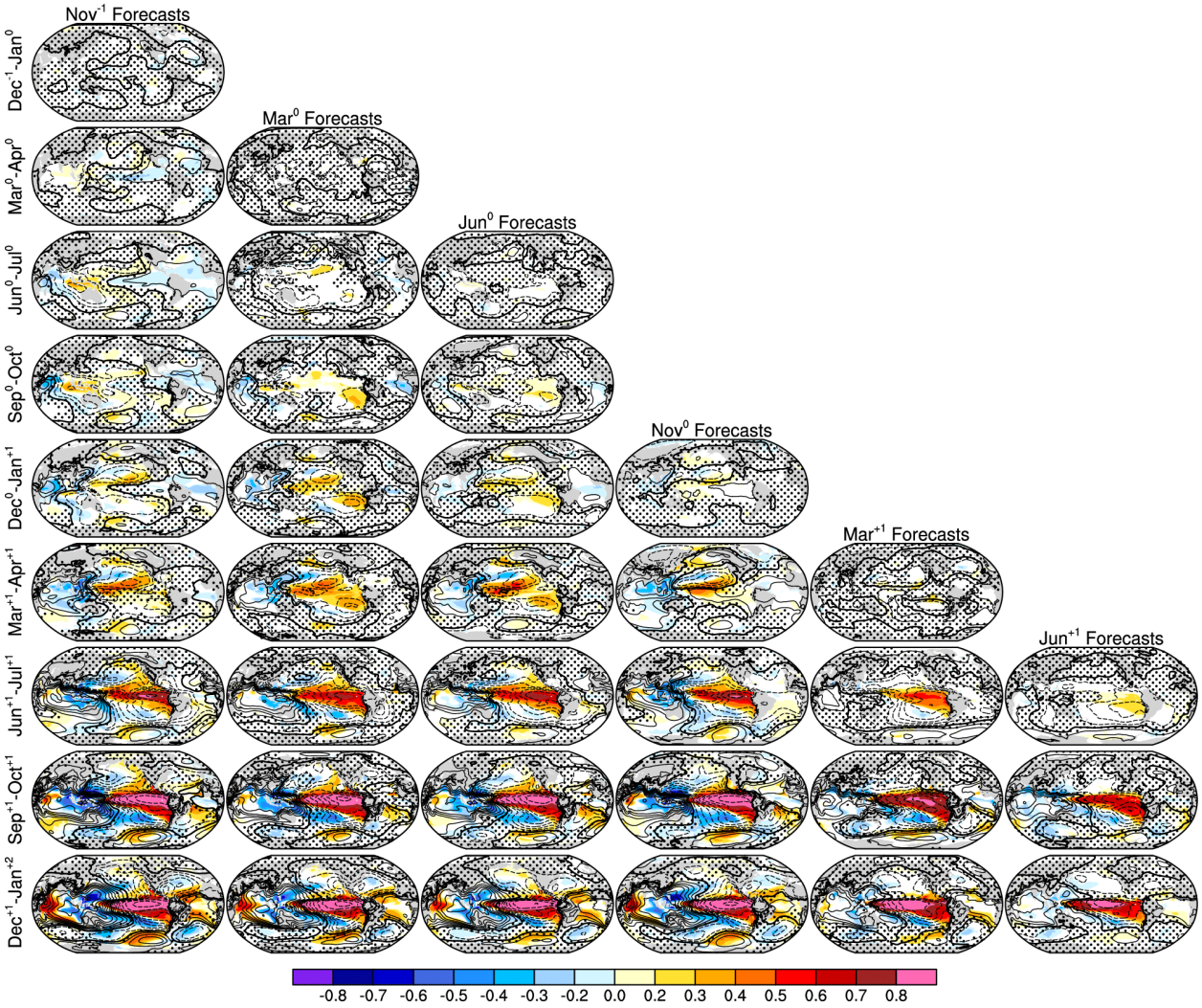

Figure S8. As in Fig. 10, but only SST correlations statistically significant at 95% confidence levels are shown. The insignificant SLP correlations are masked by stipples.